Acta Crystallographica Section B
Structural Science
ISSN 0108-7681

Longitudinal positional ordering of *n*-alkane molecules in urea inclusion compounds

Thomas Weber,*† Hans Boysen and Friedrich Frey

Institut für Kristallographie und Angewandte Mineralogie, Ludwig-Maximilians-Universität München, Theresienstrasse 41, D-80333 München, Germany

† Present address: Laboratorium für chemische und mineralogische Kristallographie, Universität Bern, Freiestrasse 3, CH-3012 Bern, Switzerland.

Correspondence e-mail: thomas.weber@krist.unibe.ch

Received 4 January 1999
Accepted 5 August 1999

The profiles of diffuse layers, which are present in diffraction patterns of urea inclusion compounds, are interpreted quantitatively by a longitudinal positional *paracrystalline* order of the alkane guest molecules within the channels of the urea-host framework structure, in agreement with the expected behaviour of a one-dimensional system. With decreasing temperature there is a gradual transition into long-range order behaviour. This ordering process remains unaffected by structural changes related to lateral correlations within and between both host and guest substructures, including a structural phase transformation. The differing behaviour of a mixed system (pentadecane/hexadecane) with average period almost commensurate with the urea host lattice is explained by the superposition of main and satellite layers. The distribution of both molecules within each tunnel is random.

1. Introduction

Urea inclusion compounds (UICs) are interesting systems for studying interactions and ordering processes in molecular crystals. Basically they consist of a honeycomb-like urea host structure with a quasi-hexagonal lattice, forming open tunnels parallel to **c** in which various long-chain molecules (here, *n*-alkanes C_nH_{2n+2}, abbreviated C*n*) are embedded as guests. UICs belong to the class of composite crystals, where host and guest substructures have different translational and/or point symmetry. In particular, they show complex disorder phenomena for various reasons: (i) both substructures have a different 'dimensionality', *viz.* in the 'tubes' of the three-dimensional ordered urea-host framework, a predominately one-dimensional guest structure, the alkane chains, are embedded; (ii) the orthorhombic or monoclinic *eigen* symmetry of the alkane molecules is in competition with the hexagonal symmetry of the urea host structure; (iii) both substructures have – along the unique axis – non-matching, in general incommensurate, translational periods $c_{h(\mathrm{ost})}$ and $c_{g(\mathrm{uest})}$. An exception is the mixture C15/C16 for which, to a very good approximation, $c_g = 2c_h$, where we have an almost commensurability in a statistical sense. Since the host framework collapses after removing the guests from the tunnels (McAdie, 1962), there have to be significant interactions between both substructures. These interactions are responsible for frustrations which become evident from mutual (incommensurate) modulations and disordering. It is also quite understandable that the ordering behaviour is highly temperature dependent, including possible structural phase transformations.

The basic structural features of the host and guest structures are reflected by typical diffraction patterns (*cf.* Fig. 1): sharp

Bragg reflections of the three-dimensional urea host and narrow diffuse layers ('*s*-layers') perpendicular to the *c*-axis corresponding to the one-dimensional guest structure. As the *s*-layers show some intensity modulations and are superimposed by weak Bragg-like reflections, however, this rough subdivision is not fully adequate, and lateral correlations between the guest molecules cannot be neglected (Forst *et al.*, 1987; Fukao, 1994*a*,*b*; Weber, Boysen, Honal *et al.*, 1996). In addition, mutual modulations of host and guest lattices give rise to three-dimensional and one-dimensional satellite scattering accompanying the Bragg reflections and the *s*-layers, respectively (Fig. 2). For UICs with *n*-alkanes as guest molecules, the intensity of satellite scattering increases with decreasing temperature. A more detailed qualitative description and interpretation of the satellite scattering is given by Weber, Boysen, Honal *et al.* (1996) and Lefort *et al.* (1996). The first refinement of the complete modulated composite structure of UIC with C17 showed that the modulation of the guest by the host is dominant at room temperature (Weber *et al.*, 1997).

Another characteristic diffuse diffraction feature of UICs is the set of so-called '*d*-bands', which are completely diffuse perpendicular to **c*** and also broadened parallel to **c*** (Fig. 1). From their positions and widths they can be related to a maximum of the form factor of the alkanes and, in consequence, explained by a longitudinal and lateral disorder of the guest molecules which was previously assumed to be an intramolecular disorder of the alkanes (Forst *et al.*, 1987) or a result of random displacements of the molecules within the channels (Welberry & Mayo, 1996). At low temperatures UICs with *n*-alkanes undergo a phase transition from a structure with hexagonal symmetry (space group $P6_122$) to an orthorhombic structure (space group $P2_12_12_1$ – host only). The transition temperature T_c depends on the length of the alkanes and lies between ~120 and 160 K for the compounds discussed in this paper. The phase transition is characterized by an increasing lateral orientational correlation of the alkanes, which perform rotational diffusion around their long axis at high temperatures (Boysen *et al.*, 1988; Guillaume *et al.*, 1990; Souaille *et al.*, 1997). In the low-temperature phase the rotational motion of the alkanes is frozen in. As a consequence the alkane molecules order in (local) herringbone-like arrangements, which cause a distortion of the host structure (Chatani *et al.*, 1977, 1978; Forst *et al.*, 1986; Welberry & Mayo, 1996).

In this paper we concentrate on an analysis of the *s*-layer system. As can be seen from Fig. 1, there is no *s*-layer of zeroth order, *i.e.* the projection of the guest molecules parallel to the tunnel axis is perfectly long-range ordered. This statement does not contradict the behaviour of the mixed *commensurate* C15/C16 system at low temperatures where a 'zeroth' *s*-layer is clearly visible (Fig. 3). In contrast to incommensurate structures the mutual modulations of commensurate subsystems also depend on their relative phases. Thus, the projection of the structure parallel to the modulation vector may vary for different channels, if the relative *z*-position of the guest structure to the host is not the same (*e.g.* for transverse modulations). From the point of view of a higher dimensional description of the composite structure the zeroth diffuse layer can be related to a superposition of different *s*-satellite layers with $l\mathbf{c}_h^* + m\mathbf{c}_g^* = 0$, where l and m refer to the (satellite-) indices of host and guest structures parallel to the unique axis. For further details about *s*-satellite layers in UICs, see Weber, Boysen, Honal *et al.* (1996). Another explanation for the existence of a diffuse zeroth layer would be that different tunnels do not contain the same number of C15 or C16 molecules. However, in that case the resulting diffuse scattering is not expected to appear only at very low temperatures. Thus, this model is not very likely.

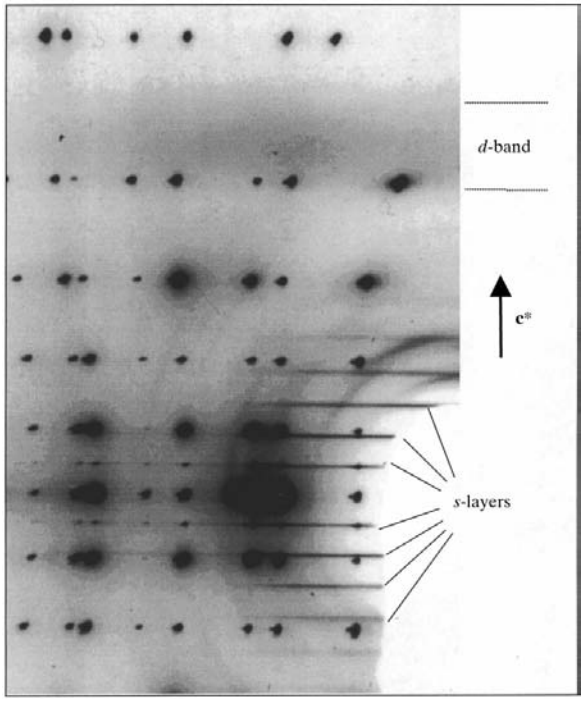

Figure 1
Typical oscillation photograph of UICs (here, urea/heptadecane). The strong Bragg reflections are mainly caused by the host structure, while the *s*-layers and the *d*-band correspond to the disordered guest system. Oscillation range: ±30°, Cu $K\alpha_1$ radiation, room temperature.

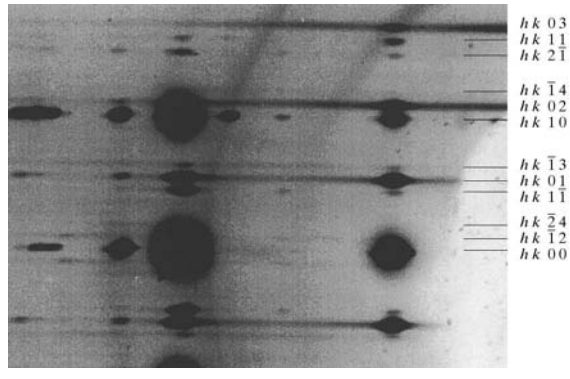

Figure 2
Satellite scattering in UIC with tetradecane. Indices refer to a (3 + 1)-dimensional (modulated) composite structure of C14. Oscillation range: ± 20°, Cu $K\alpha_1$ radiation, T = 40 K.

Up to now it has generally been assumed that the *s*-layers are as sharp as Bragg reflections parallel to **c***. Therefore, it was concluded that the positions of the guest molecules are long-range ordered parallel to the channel axis within each channel (Forst *et al.*, 1987; Fukao, 1994*a*,*b*), while there is complete disorder between the channels. A first hint that this may not be true in a strict sense was noticed by Weber, Boysen, Honal *et al.* (1996). A similar observation has recently been reported with neutrons (Lefort, 1998); however, uncertainties with the deconvolution of the resolution function did not allow definite conclusions to be drawn. This is an important problem because for a strictly one-dimensional system no long-range order can exist above $T = 0$ K, and fluctuations should lead to a broadening of the diffuse layers (= one-dimensional Bragg peak) with increasing momentum transfer. Therefore, in this paper we present a high-resolution synchrotron study of the widths of the *s*-layers and investigate the temperature-dependent longitudinal positional disorder of the guest molecules.

The compounds urea + tetradecane (C14), urea + heptadecane (C17), and the mixed-guest system urea + (pentadecane/hexadecane) (C15/C16), with a ratio C15:C16 = 1:1, were investigated to compare the behaviour of guest molecules with different lengths and the behaviour of mixed and unmixed guest systems. As the average molecular length of the mixed system C15/C16 is commensurate with the translational period of the host parallel to **c** to a good approximation ($\bar{c}_{C15/C16} = 2c_{host}$), this mixed system is of special interest for deciding whether or not an ordering of the guests occurs, either due to the (global) distribution of the two types of molecules or due to the (local) positions of individual alkanes relative to their neighbours.

2. Experimental

2.1. Crystal growth

The crystals were grown from a saturated solution of urea and alkanes in 2-propanol. The solution was slowly cooled from 318 K to room temperature within about 2 weeks. The final samples used for the synchrotron experiments were needle-like crystals with hexagonal prismatic shape, which had a length of several millimetres parallel to **c** and a diameter of ~0.6 mm for C14 and C15/C16 and 0.9 mm for C17.

2.2. Synchrotron measurements

Measurements were carried out with a Weissenberg camera used in oscillation mode installed at the beamline G3 of the synchrotron source HASYLAB/DESY (Hamburg). A wavelength $\lambda = 1.5602$ Å was used. The camera is designed for experiments at low temperature with low background (Adlhart & Huber, 1982). The cooling device of the camera is a closed-cycle helium cryostat. The specimens were contained in an evacuated Be cylinder. The radius of the camera was 41.5 mm. The *c*-axis was oriented parallel to the rotation axis which was perpendicular to the impinging X-ray beam. To have a high resolution parallel to **c***, an additional adjustable slit was mounted in order to limit the horizontal width of the primary beam to a few tenths of a millimetre. In order to obtain a sufficiently large number of Bragg reflections for the determination of the resolution function, the oscillation range for C17 was ±30°. Because of significant diffuse scattering surrounding the Bragg reflections, however, large regions of the *s*-layers could not be examined. Thus, the oscillation range of the other compounds was limited to ±10°. The exposure time was between 30 and 90 min, depending on the crystal size and the intensity of the primary beam. A flexible imaging plate was used as a detector. The imaging plates were read out on an imaging-plate scanner at the highest sensitivity and maximum resolution (88 μm pixel^{-1}). Owing to unknown parameters the measured intensities were not corrected for the dead time of the scintillation counter of the imaging-plate scanner. However, as the intensities of the diffuse phenomena were comparably low and covered only a small part of the dynamic range (~5–10% of saturation), it can be assumed that, to a good approximation, a linear relationship between measured and true intensities is obeyed. In particular, the widths of the diffuse layers should not be affected by saturation effects.

3. Theory

For the description of the distribution of the guest molecules in the inclusion compounds C14 and C17 and for the corresponding diffraction patterns we follow a theory which was introduced by Zernike & Prins (1927) to describe the scattering by one-dimensional liquids, and which was extended for solids ('paracrystals') by Hosemann (1950*a*,*b*,*c*). Within these models only correlations between neighbouring particles (here, molecules) are assumed to be effective leading to a liquid-like distribution of the molecules. In the case of a one-dimensional crystal the scattering intensity of such a distribution is given by (see, for example, Vainshtein, 1966)

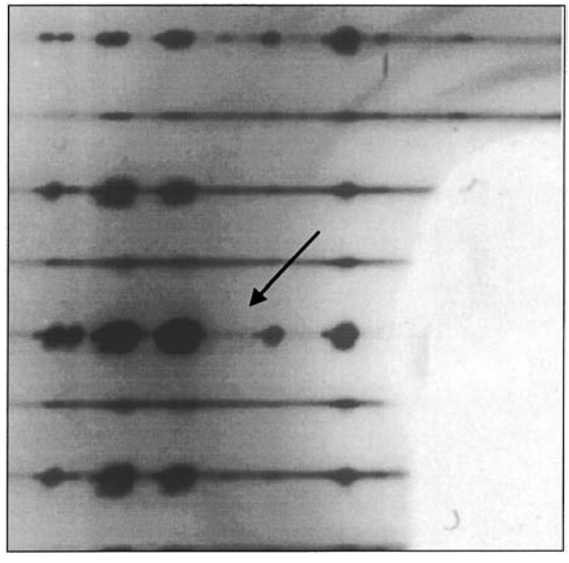

Figure 3
Oscillation photograph showing the *s*-layer of 'zeroth order' (arrow) of the system C15/C16. Oscillation range: ±30°, Cu $K\alpha_1$ radiation, $T = 40$ K.

$$I(Q_l) = \frac{1 - F(Q_l)^2}{1 - 2F(Q_l)\cos(2\pi Q_l \bar{c}) + F(Q_l)^2}, \quad (1)$$

where $F(Q_l)$ is the real part of the Fourier transform of the correlation function of neighbouring molecules/particles and $\bar{c}$ is the average distance between the c.o.m.s (centre of mass) of two molecules. If the correlation function of neighbouring molecules can be described by a Gaussian

$$H_1(z) = (2\pi)^{-1/2}\Delta^{-1}\exp\left[-(z-\bar{c})^2/2\Delta^2\right], \quad (2)$$

the corresponding Fourier transform $F(Q_l)$ is given by

$$F(Q_l) = \exp(-2\pi^2 Q_l^2 \Delta^2) \simeq 1 - 2\pi^2 Q_l^2 \Delta^2, \quad (3)$$

where Δ is the disorder parameter for the paracrystal model. For not too large values of $Q_l\Delta$, (1) is a good approximation to a Lorentzian with maxima very close to integer values of $l = Q_l\bar{c}$ and the widths increase quadratically with Q_l according to

$$\mathrm{FWHM}(Q_l) = (\pi^2\Delta^2/\bar{c})Q_l^2. \quad (4)$$

In contrast to compounds with molecular guests of only one species, the positional distribution of the alkanes in the C15/C16 compound depends not only on the effects, which were discussed previously, but also on the distribution of the two types of guest molecules. In principle, the expected diffuse scattering of such a disorder problem has already been investigated by Hendricks & Teller (1942). Here it will be discussed in more detail for the situation in the C15/C16 compound including the positional disorder. As a starting point we assume that, on average, we have an equal number of pentadecane and hexadecane molecules within each urea host channel. Furthermore, we assume that the alkanes are close packed and all molecules are in a long-stretched *all-trans* conformation. The Patterson function of such a distribution can be derived as follows. For an arbitrary position z_0 in a channel we have the same probability of finding a pentadecane molecule of length c_{15} or a hexadecane molecule of length c_{16}. Then the position of the nearest neighbour in the positive direction is given by $z_{1,0} = c_{15}$ and $z_{1,1} = c_{16}$ with probabilities of $p_{1,0} = 0.5$ and $p_{1,1} = 0.5$, respectively. Now the positions of the next nearest neighbours is either $z_{2,0} = 2c_{15}$ ($p_{2,0} = 0.25$) or $z_{2,1} = c_{15} + c_{16} = 2\bar{c}$ ($p_{2,1} = 0.5$) or $z_{2,2} = 2c_{16}$ ($p_{2,2} = 0.25$). Generally, this distribution can be described by a binomial distribution where the position of the nth neighbour is given by

$$z_{n,k} = (n-k)c_{15} + kc_{16}. \quad (5)$$

The equivalent positions in the opposite c-direction are given by

$$z_{-n,k} = -z_{n,k}. \quad (6)$$

$p_{n,k}$ is given by the normalized binomial coefficient

$$p_{n,k} = \binom{n}{k} 2^{-n}. \quad (7)$$

A description of such a distribution in terms of a paracrystalline arrangement can be expressed by the correlation function of neighbouring molecules $H_1(z)$,

$$H_1(z) = \begin{cases} 0.5 & \text{for } z = c_{15} \text{ and } z = c_{16} \\ 0 & \text{elsewhere} \end{cases}. \quad (8)$$

If we take into account the longitudinal positional disorder as discussed previously, we can express the distribution function by a convolution of $H_1(z)$ with a Gaussian function

$$H_1'(z) = H_1(z) * (2\pi)^{-1/2}\Delta^{-1}\exp(-z^2/2\Delta^2). \quad (9)$$

Again equation (1) holds for the scattering intensity of such a distribution, where $F(Q_l)$ is the real part of the Fourier transform of $H_1' = (z + \bar{c})$. Defining $c_\Delta = c_{16} - c_{15}$, the Fourier transform of (8) shifted to its centre of gravity is given by

$$\mathcal{F}[H_1(z+\bar{c})] = \left\{\tfrac{1}{2}\cos[2\pi Q_l(c_\Delta/2)] + \tfrac{1}{2}\cos[-2\pi Q_l(c_\Delta/2)]\right\}.$$

With the convolution theorem and with (3) we obtain

$$\begin{aligned} F(Q_l) &= \left[\tfrac{1}{2}\cos(\pi Q_l c_\Delta) + \tfrac{1}{2}\cos(-\pi Q_l c_\Delta)\right] \\ &\quad \times \exp(-2\pi^2 Q_l^2\Delta^2) \\ &= \cos(\pi Q_l c_\Delta)\exp(-2\pi^2 Q_l^2\Delta^2). \end{aligned} \quad (10)$$

For $F(Q_l) > 0$, $I(Q_l)$ has maxima close to integer values of $l = Q_l\bar{c}$ and minima near $l = (2n+1)/2$ (n = integer), and *vice versa* if $F(Q_l) < 0$. With $F(Q_l) \simeq 0$ the maxima are very broad and overlapping (Fig. 4). As the sign of $F(Q_l)$ is given by the cosine function, the first shift of the maxima from integer l to positions with $l = (2n+1)/2$ should occur at $Q_l c_\Delta \simeq 0.5$, *i.e.* in the region of the first d-band. This could not be checked directly since no measurements beyond the first d-band were performed.

The half-widths of slightly overlapping maxima can be approximated by the ratio of their integral and maximum intensity. Following Vainshtein (1966) the widths of the maxima of (1) are given by

$$\mathrm{FWHM}(Q_l) = (2\bar{c})^{-1}[1 - F(Q_l)]. \quad (11)$$

It should be pointed out that the derivation of this equation implies that the maxima of intensities are at integer values of l and the minima are located at $l = n/2$ (n = odd), *i.e.* for

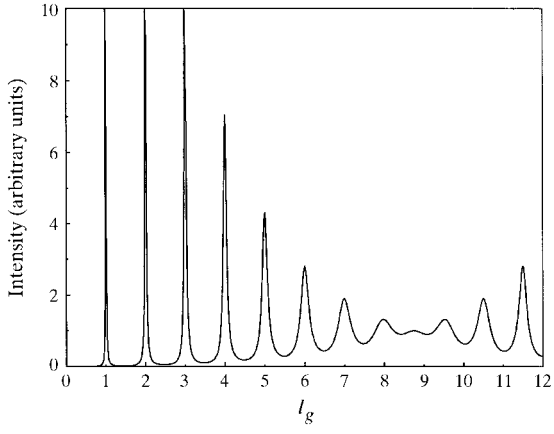

Figure 4
Intensity profile across the *s*-layers of C15/C16 after (1) and (10) for random distribution of the pentadecane and the hexadecane molecules and $\Delta = 0$.

$\cos(\pi Q_l c_\Delta) > 0$, which is fulfilled for all examined *s*-layers. Using (10) we obtain the half-widths of the *s*-layers for a mixed compound,

$$\begin{aligned}\mathrm{FWHM}(Q_l) &= (2\bar{c})^{-1}[1 - F(Q_l)] \\ &= (2\bar{c})^{-1}[1 - \cos(\pi Q_l c_\Delta)\exp(-2\pi^2 Q_l^2 \Delta^2)].\end{aligned} \tag{12}$$

Comparing (12) with (4) we see that, for the same values of Δ, the *s*-layers of the mixed guest system are broader than the *s*-layers of the unmixed guest system as long as $\cos(\pi Q_l c_\Delta) < 1$.

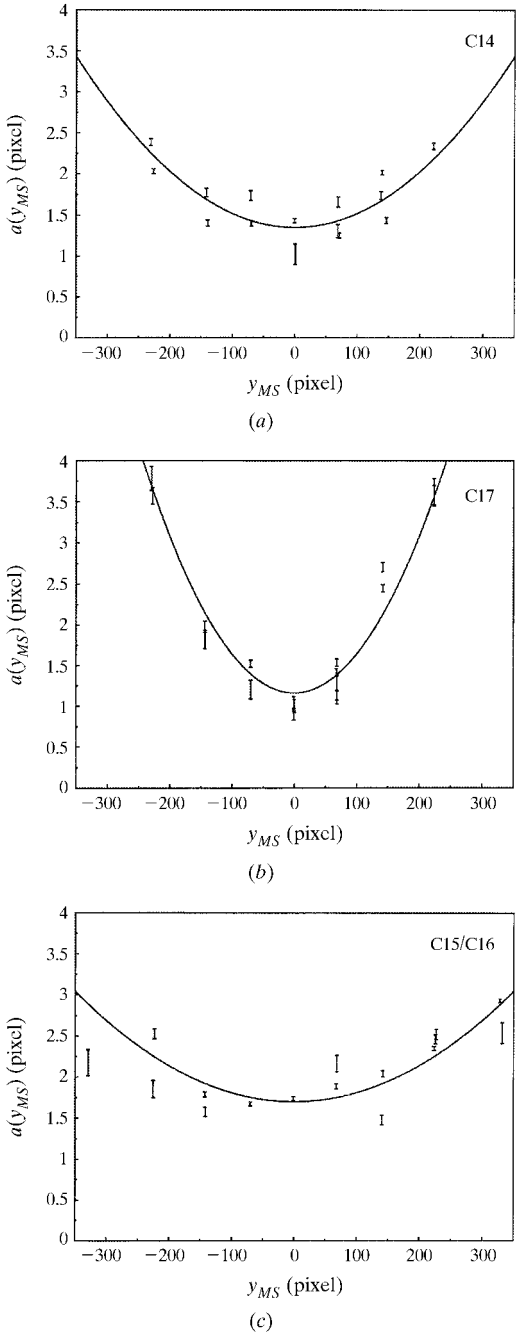

Figure 5
Resolution parameter a_R as a function of y_{MS} from room-temperature measurements of (*a*) C14, (*b*) C17 and (*c*) C15/C16.

4. Data evaluation and results

To enhance the intensities the profiles of the *s*-layers were determined by integration along straight lines perpendicular to **c*** over a range of ~10–20 pixels at several regions of the *s*-layers with constant background. For each *s*-layer two to eight profiles could be extracted. This procedure and the determination of experimental parameters, such as orientation and position of the diffraction pattern relative to the coordinate system of the imaging plate, were performed using the program *dwb* (Weber, 1998). The standard uncertainties (s.u.'s) of the measured intensities were determined by a statistical analysis of the background scattering. It was found that $\sigma(I)$ is almost constant for background intensities, the magnitudes of which are comparable with those of the diffuse scattering, *i.e.* it is mostly affected by a (constant) intrinsic noise of the imaging-plate scanner. Therefore, all intensities were given the same weight.

As we are particularly concerned with a quantitative evaluation of the widths of the diffuse layers, the measured profiles have to be corrected (deconvoluted) for resolution effects. As a consequence of the cylindrical shape of the detector, only the zeroth layer falls normally onto the image plate. Thus, the deconvoluted widths of the *s*-layers have to be corrected for that effect too. This is performed by a transformation of the widths from coordinates of the detector to coordinates of reciprocal space (see below). In order to determine the experimental resolution function the profiles of several Bragg reflections were examined close to the positions of the *s*-layers. Again the profiles were integrated perpendicular to **c***. In order to avoid problems due to saturation effects, only reflections with a maximum intensity comparable with the diffuse intensities of the *s*-layers were used. The recorded profile of a diffraction signal is given by the convolution of its true physical shape with the instrumental resolution function (RF), which can be obtained from the profiles of Bragg reflections (assumed to be δ-functions). In the present case only the projection of the RF onto **c*** has to be taken into account. It was found that this can best be described by a convolution of a box function of width d_s and a Lorentzian with a full width at half-maximum a_R. As the box function can be related to the extension of the primary beam parallel to **c**, d_s can be assumed to be independent of y_{MS}.[1] Thus, the profiles of the Bragg reflections along **c*** as a function of y_{MS} can be described by the following – not normalized – function,

$$\begin{aligned}R(y_{MS}) &= \int_{-d_s/2}^{d_s/2} \left\{1 + \left[\frac{y_{MS} - Y}{(1/2)a_R(y_{MS})}\right]^2\right\}^{-1} \mathrm{d}Y \\ &= a(y_{MS})\left\{\arctan\left[\frac{d_s/2 + y_{MS}}{(1/2)a_R(y_{MS})}\right]\right. \\ &\quad \left. - \arctan\left[\frac{-d_s/2 + y_{MS}}{(1/2)a_R(y_{MS})}\right]\right\}.\end{aligned} \tag{13}$$

[1] x_{MS} and y_{MS} are the coordinates on the imaging plate, where x_{MS} denotes the position parallel to the equator line and y_{MS} is a coordinate parallel to the rotation axis. x_{MS} and y_{MS} are given in pixel units (1 pixel = 88 μm).

In order to determine the resolution parameters d_s and $a_R(y_{MS})$, this function was fitted to the profiles of the Bragg reflections. Generally, a good agreement between measured and fitted profiles could be achieved. As expected, for a fixed width of the primary slit, d_s shows no significant variation as a function of y_{MS}. With the exchange of the samples, the primary slit had to be re-adjusted and thus d_s was not constant (d_s = 2.8 pixels for measurements with C14, 2.1 pixels for C17 and 3.3 pixels for C15/C16). $a_R(y_{MS})$ was found to increase quadratically with increasing y_{MS} to a good approximation (Fig. 5). Thus, $a_R(y_{MS})$ can be described by the relation $a_R(y_{MS}) = l_1 y_{MS}^2 + l_2$. The resolution parameters l_1 and l_2 were determined for each temperature by fitting a parabola to the experimental data. As for d_s they did not vary significantly for the measurements of one compound. For C17 a steeper slope of $a_R(y_{MS})$ can be observed, which can be explained by the larger size of the crystal. Although some significant deviations of the experimental data from the parabola are obvious, it can be concluded that the resolution function could be determined with an accuracy of a few tenths of a pixel.

Assuming another Lorentzian L_s to describe the intrinsic profile of the *s*-layers (see above), the corresponding widths $a_s(y_{MS})$ were refined by fitting the data to the convolution product $R(y_{MS}) * L_s(y_{MS})$, which was calculated numerically.

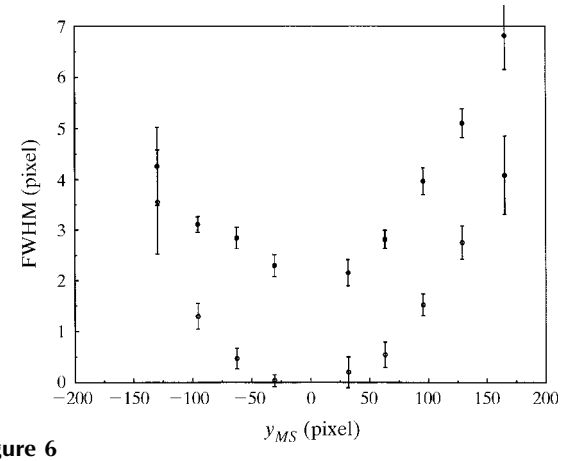

Figure 6
Influence of resolution effects on the measured half-widths of the *s*-layers (UIC/C17 at room temperature). The upper and lower values give the measured and corrected widths, respectively (see text).

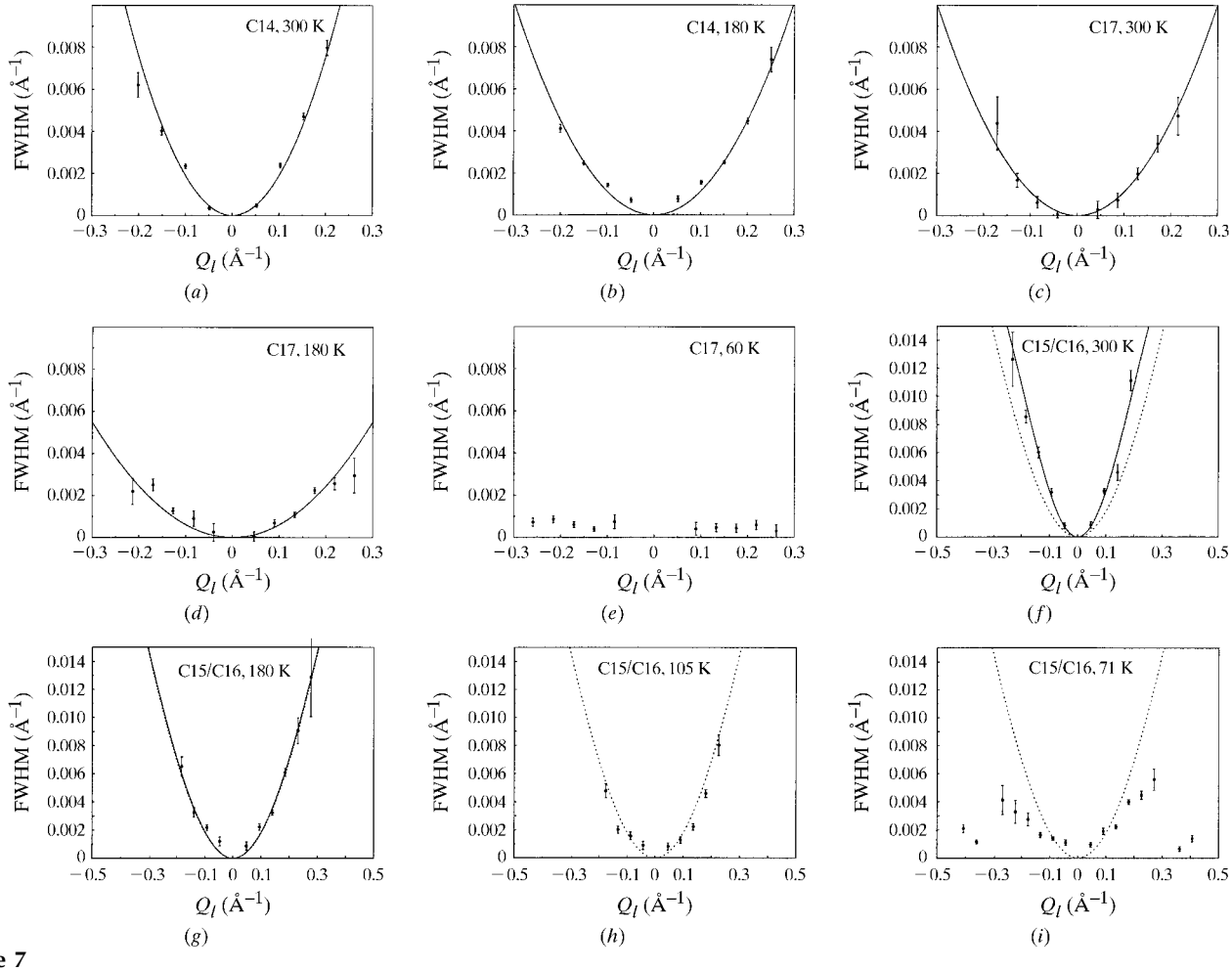

Figure 7
Widths of the *s*-layers of the investigated compounds at selected temperatures. For C14 (*a*, *b*) and C17 (*c*, *d*, *e*) a parabola is fitted to the experimental values. For C15/C16 (*f*, *g*, *h*, *i*) the dotted line gives the expected widths for $\Delta = 0$ (see text), while the solid line at 300 (*f*) and 180 K (*g*) shows the fit of (12) to the experimental results. At 180 K the dotted line and the solid line are almost superimposed. Note the different scales for C14 and C17 on the one hand and C15/C16 on the other.

Again a good agreement between measured and fitted profiles could be achieved. No significant variation of the widths of the profiles as a function of x_{MS} could be observed, *i.e.* the widths of the *s*-layers are independent of the lateral distribution. The influence of the instrumental resolution on the measured width of the *s*-layers is illustrated in Fig. 6.

The coordinates y_{MS}, in particular the widths of the *s*-layers, were transformed into reciprocal space units using the expression

$$Q_l = \left[y_{MS}/(r^2 + y_{MS}^2)^{1/2}\right]\lambda^{-1}, \qquad (14)$$

where Q_l is the position of the *s*-layer along $\mathbf{c}^*$ in units of Å^{-1} and r is the radius of the camera in pixel units. Finally, for each *s*-layer the weighted mean of the various data sets was calculated. Some representative results are shown in Fig. 7. If we assume a maximum systematic error for the widths of the *s*-layers to be $\Delta y_{MS} = 0.3$ pixels (*cf.* Fig. 5), then its influence on the transformed widths can be estimated to be $\Delta Q_l = \Delta y_{MS}/r\lambda \simeq 0.0004$ Å^{-1} for small y_{MS} [*cf.* (14)], *i.e.* for *s*-layers of low scattering order. For *s*-layers of higher order this value is even smaller. Compared with the results shown in Fig. 7, it can be seen that the maximum systematic error by an improper resolution correction is significant only for very narrow *s*-layers.

5. Discussion

The UICs with C14 or C17 and with the C15/C16 mixture show a remarkably different behaviour and will therefore be discussed separately.

5.1. UIC with C14 and C17

As shown in Fig. 7 the observed widths of the *s*-layers can be described well by (4), *i.e.* by a quadratic increase of the widths as a function of l, except for C14 at low temperatures where the widths show significant deviations from a parabolic behaviour at low Q_l (*cf.* Fig. 7*b*). Only Δ was refined by fitting a parabola to the observed widths, while $\bar{c}$, the average translational distance of the guest molecules, was fixed using the corresponding room-temperature value (Lenné *et al.*, 1970). In the case of C17 the average distance of the alkanes at low temperatures (20 K) is ∼0.2 Å, *i.e.* ∼1%, shorter than the room-temperature value. This deviation is therefore negligibly small compared with the s.u.'s of the Δ values which are ∼10%. Fig. 8 shows the temperature dependence of Δ for the investigated compounds.

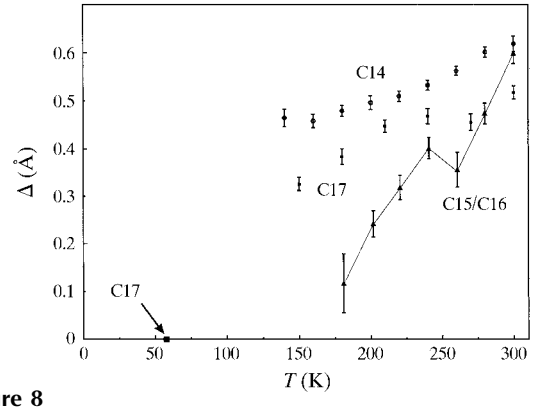

Figure 8
Variation of Δ as a function of temperature and of the guest molecules. The line connecting the values of C15/C16 serves as a guide to the eye only.

Δ decreases continuously with decreasing temperature in the case of the non-mixed guest systems. The values for C14 are slightly higher than those of C17. For C17 it was possible to measure the widths of the *s*-layers at two temperatures within the low-temperature phase (150 and 60 K; $T_c \simeq 160$ K). No anomalous behaviour of Δ could be observed around the phase transition. At 60 K the *s*-layers (C17) are almost sharp and show no variation with increasing scattering order. Unfortunately, owing to experimental problems it was not possible to measure the widths for UIC + C14 below T_c.

These results can be interpreted in terms of two different models, described below.

Model (1): the lengths of the alkane molecules stay constant with temperature, while the distances between the molecules fluctuate and can be described by Gaussian distribution functions. The experimental results can be explained very well by this model: the mobility of the alkanes decreases with increasing molecular length and decreasing temperature. The magnitude of Δ roughly coincides with values obtained from different investigations of the translational dynamics, *e.g.* the translational diffusion lengths determined by quasielastic neutron scattering (El Baghdadi *et al.*, 1993).

Model (2): the lengths of the molecules vary according to a Gaussian distribution. From spectroscopic studies it is known that alkane guest molecules show a significant intramolecular disorder, which decreases with decreasing temperatures (Casal, 1990; Imashiro *et al.*, 1988; El Baghdadi *et al.*, 1996). Torsions of the whole molecule and partial *gauche* conformations, especially at the end positions of the molecules, have been observed. As the molecules exhibit their maximum lengths in an undistorted *all-trans* conformation, it can be concluded that the length of a molecule and, with this, the distribution of the molecules, are a function of intramolecular disorder. Again the observed behaviour of Δ as a function of molecule length and temperature could be explained by this model. From a crystal chemical point of view, however, model (1) would provide unfavourable large gaps between the alkanes along the *c*-axis, which gives some preference for model (2). In general, however, a combination of both mechanisms cannot be excluded.

The slight broadening of *s*-layers of low scattering order of the system C14 at low temperatures (see Fig. 7*b*) may be explained by a longitudinal (one-dimensional) domain structure of the guest molecules due to interruptions caused by partial commensurations with the host. This effect is absent in UIC(C17). An explanation might be given by the assumption that, for C17, host and guest structures are almost commensurate parallel to **c** and, therefore, longer-range ordered structures parallel to **c** may be favoured. However, an insuf-

ficient resolution correction cannot be excluded as another explanation.

As the *s*-layers in UIC(C17) show no anomalous behaviour in the low-temperature phase, it can be concluded that the longitudinal correlations of the alkanes remain more or less unaffected either by the lateral deformation of the host structure or by the freezing of the rotational degree of freedom of the guest molecules around their long axes.

For C17 the room-temperature widths of the *s*-layers were previously measured at the synchrotron source ESRF (Grenoble) using a four-circle diffractometer (Weber, Boysen, Frey *et al.*, 1996). The data evaluation gave a higher value for Δ [0.71 (5) Å compared with 0.52 (1) Å]. The deviation may be explained by an insufficient resolution correction. Owing to limited experimental time, most of the resolution parameters could not be measured and had to be estimated.

The existence of weak Bragg-like reflections on the *s*-layers (*cf.* Fig. 1) seems to be in contradiction with the paracrystalline model of the guest molecules distribution. If they were completely sharp parallel to **c*** then we would indeed have to take into account a long-range ordered structure parallel to **c**. In that case the positional correlation between the guest molecules would not be lost completely for long distances. The driving force may be due to partial commensurations between host and guest. Unfortunately, from the experimental evidence it could not be decided unambigously if they have the same widths as the *s*-layers or not, since they appear only on very narrow *s*-layers, where the width of both diffraction phenomena are below the experimental resolution. However, if the reflections were really sharp, the corresponding effect must be very weak, as the intensities decrease rapidly parallel to **c***. Thus, we can safely assume that additional long-range-order terms should have no significant influence on the short-range correlations of the guest molecules, as described in this paper. As mentioned before, the sharpness of these reflections perpendicular to **c*** only indicates that the guests have a good correlation in lateral directions, *i.e.* independent from their longitudinal distribution. Another interpretation would be that these reflections are sharp satellites from the modulation of the host by the guest. Here, however, it is not expected that the modulation is long-range ordered if the guest structure itself is not. Thus, the satellites should show the same widths as the corresponding main diffraction phenomena of the guest (see also Fig. 9 and further explanations below).

5.2. UIC with C15/C16 mixture

The expected widths of the *s*-layers parallel to **c*** are given by (12). As a reference, in Figs. 7(*f*)–7(*i*) the expected behaviour of the widths of the *s*-layers is shown for $\Delta = 0$ by dotted lines, *i.e.* for a random distribution of the pentadecane and hexadecane molecules without additional displacive disorder. Additionally, for $T = 300$ K and $T = 180$ K the fit of (12) to the widths of the *s*-layers is shown by solid lines (for $T = 180$ K the dotted and solid lines are almost superimposed). For these calculations $c_\Delta = 1.277$ Å and $\bar{c} = 22.04$ Å [$\simeq (c_{15} + c_{16})/2$] (*cf.* Lenné *et al.*, 1970) were fixed. It can be concluded that in the C15/C16 system the broadening of the *s*-layers is mainly caused by the random distribution of the alkane molecules.

The refined disorder parameters Δ are shown in Fig. 8. At 300 K there is a good agreement with the results of C14 and C17. With decreasing temperature, however, Δ decreases faster than for the C14 and C17 compounds. Below 180 K, Δ values could no longer be determined since the widths of the *s*-layers are even slightly smaller than expected for $\Delta = 0$. (The exception of the 71 K measurement, where the widths show a very unusual behaviour, is discussed separately below.) Therefore, small systematic errors cannot be ruled out: apart from a not fully adequate correction of resolution effects or a slightly too large value for c_Δ, other possible explanations for this behaviour might be as follows.

(i) The assumptions made are not correct in so far as the two types of guest molecules are not distributed completely at random, or the numbers of pentadecane and hexadecane molecules within each channel are not equal. Thus, a significant correlation of the longitudinal distribution of pentadecane and hexadecane molecules could explain why *s*-layers show smaller widths than expected for a random distribution of the molecules. On the other hand, the large widths of the *s*-layers at room temperature would require a much larger Δ than in the case of C14 and C17. This does not seem to be very likely. Since the average length of the guest molecules in the C15/C16 compound is comparable with the molecular length of C14 and C17, it can be assumed that the values of Δ are not too far from those in the unmixed systems, which are found at high temperatures. Moreover, the rapid decrease of the widths of the *s*-layers with decreasing temperatures and of *s*-layers of higher scattering order at 71 K is difficult to explain. Thus, a

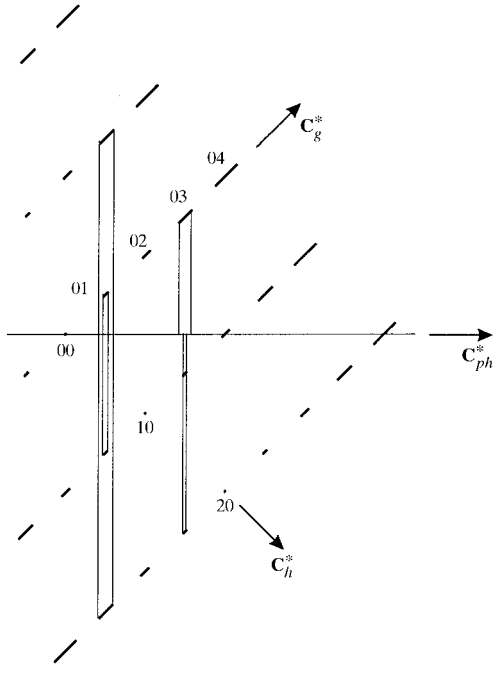

Figure 9
Representation of $\mathbf{c}_g^*$ and $\mathbf{c}_h^*$ in a reciprocal superspace approach for the C15/C16 compound.

random distribution of the alkane molecules still seems to be most plausible.

(ii) The main *s*-layers overlap with satellite *s*-layers. The deviation at low temperatures, in particular at 71 K, can be well explained, as follows. As mentioned above, UICs show satellite *s*-layers of increasing intensity with decreasing temperatures (Weber, Boysen, Honal *et al.,* 1996). As the C15/C16 system is an almost commensurate one, main *s*-layers and satellite *s*-layers are superimposed. It may be assumed that satellite *s*-layers of satellite index *m* show the same width as main *s*-layers of the *m*th order. Since the intensities of the satellite *s*-layers increase with decreasing temperatures, the superposition of satellite *s*-layers with main *s*-layers becomes more and more important when the crystal is cooled down. This means that the apparent widths of broad main *s*-layers of high order are *decreased* by the superimposed sharp satellites of lower indices and, *vice versa*, the widths of sharp main *s*-layers of low order are *increased* by the superposition of broad satellites of higher indices. Fig. 9 illustrates the situation in a superspace approach. The observed diffraction pattern of a higher-dimensional reciprocal lattice is given by a projection of the sublattices onto the physical reciprocal space ($\mathbf{c}_{\rm ph}$*). The indices l, m refer to the main reflections of both subsystems. As an example, the main *s*-layer $0, 1$ is superimposed by the satellite layer $1, \bar{1}$ with the same width and by the satellite layers $2, \bar{3}$ and $\bar{1}, 3$ with increased widths. On the other hand, the main layer $0, 3$ is superimposed by the narrow satellites $1, 1$ and $2, \bar{1}$. Of course, the layer $0, 3$ is also superimposed by broad satellites with higher indices but, as we know from the theory of modulated structures, their intensities decrease rapidly with increasing distance from $\mathbf{c}_{\rm ph}$*. Therefore, we can safely assume that the influence of these layers is negligible compared with the narrow ones. This effect is most pronounced in the range of the first *d*-band ($l_{\rm guest(C15/C16)} = 8$, 9). For C14 and C17, only very weak main *s*-layers could be observed, while with C15/C16 the *s*-layers in this region are strong and almost sharp. Thus, it can be safely concluded that these intensities are mainly due to satellite scattering with low satellite indices.

In addition, the increasing widths of *s*-layers of low order at low temperatures may also be explained by a longitudinal domain structure of the alkanes as discussed for the C14 system.

6. Conclusions

At high temperatures, *i.e.* around room temperature, the longitudinal order is mainly governed by intramolecular disorder and direct alkane–alkane nearest-neighbour interactions with a paracrystalline behaviour. The ordering is largely unaffected by the structure of the surrounding urea host channels. This is confirmed by the observation that the widths of the diffuse *s*-layers remain unaffected by passing through the transition temperature where host and guest structure show significant structural changes. In consequence, we have a 'true' one-dimensional guest substructure. There is no complete long-range order along the unique axis, which indicates the dominant influence of entropic terms.

By lowering the temperature there is a gradual change towards a one-dimensional long-range order of the guest molecules. This corresponds to the behaviour of the intensities of the satellite scattering (Weber, Boysen, Honal *et al.* 1996; Lefort *et al.*, 1996) which become stronger with lower temperatures and which are also almost unaffected by passing through the transition temperature. On the other hand, it does indicate a remarkable influence of host–guest interactions on the longitudinal ordering of the guest at low temperatures. In the special case of the UIC + C15/C16 system a random distribution of C15 and C16 molecules in the channels was found. This result seems to be plausible, since the distribution is irreversibly introduced during the growth process and a rearrangement of the molecules is not likely to occur for steric or kinetic reasons. If the interactions between host and guest structure would play the decisive role for the longitudinal ordering process at high temperatures, one should expect a more or less regular alternating sequence C16, C15, C16, C15 *etc.* which would match the host structure more closely. The present analysis together with previous results shows that longitudinal and lateral (rotational) ordering processes are largely decoupled in UICs. This is in agreement with recent findings from quasielastic Brillouin scattering (Ollivier *et al.*, 1998).

This work was supported by funds from the Deutsche Forschungsgemeinschaft under Fr 747/7-1.

References

Adlhart, W. & Huber, H. (1982). *J. Appl. Cryst.* **15**, 241–244.
Boysen, H., Frey, F. & Blank, H. (1988). *Mater. Sci. Forum*, **27/28**, 123–128.
Casal, H. (1990). *J. Phys. Chem.* **94**, 2232–2234.
Chatani, Y., Anraku, H. & Taki, Y. (1978). *Mol. Cryst. Liq. Cryst.* **48**, 219–231.
Chatani, Y., Taki, Y. & Tadokoro, H. (1977). *Acta Cryst.* B**33**, 309–311.
El Baghdadi, A., Dufourc, E. J. & Guillaume, F. (1996). *J. Phys. Chem.* **100**, 1746.
El Baghdadi, A., Guillaume, F., Boysen, H., Dianoux, A. J. & Coddens, G. (1993). *Quasielastic Neutron Scattering*, edited by J. Colmenero, A. Alegria & F. J. Bermejo, pp. 131–140. Singapore: World Scientific.
Forst, R., Boysen, H., Frey, F., Jagodzinski, H. & Zeyen, C. (1986). *J. Phys. Chem. Solids*, **47**, 1089–1097.
Forst, R., Jagodzinski, H., Boysen, H. & Frey, F. (1987). *Acta Cryst.* B**43**, 187–197.
Fukao, K. (1994*a*). *J. Chem. Phys.* **101**, 7882–7892.
Fukao, K. (1994*b*). *J. Chem. Phys.* **101**, 7893–7903.
Guillaume, F., Sourisseau, C. & Dianoux, A. J. (1990). *J. Chem. Phys.* **93**, 3536–3541.
Hendricks, S. & Teller, E. (1942). *J. Chem. Phys.* **10**, 147–167.
Hosemann, R. (1950*a*). *Z. Phys.* **128**, 1–35.
Hosemann, R. (1950*b*). *Z. Phys.* **128**, 46–62.
Hosemann, R. (1950*c*). *Z. Phys.* **128**, 465–492.
Imashiro, F., Kuwahara, D., Nakai, T. & Terao, T. (1988). *J. Chem. Phys.* **90**, 3356–3362.
Lefort, R. (1998). Thesis, University of Rennes, France.
Lefort, R., Etrillard, J., Toudic, B., Guillaume, F., Breczewski, T. & Bourges, P. (1996). *Phys. Rev. Lett.* **77**, 4027–4030.

Lenné, H. U., Mez, H. Ch. & Schlenk, W. Jr (1970). *Liebigs Ann. Chem.* **732**, 70–96.
McAdie, H. G. (1962). *Can. J. Chem.* **40**, 2195–2203.
Ollivier, J., Ecolivet, C., Beaufils, S., Guillaume, F. & Breczewski, T. (1998). *Europhys. Lett.* **43**, 546–551.
Souaille, M., Smith, J. C. & Guillaume, F. (1997). *J. Phys. Chem.* **101**, 6753–6757.
Vainshtein, B. K. (1966). *Diffraction of X-rays by Chain Molecules.* Amsterdam: Elsevier.
Weber, Th. (1998). Unpublished.
Weber, Th., Boysen, H., Frey, F., Berar, J. F. & Bley, F. (1996). *Z. Kristallogr. Suppl.* **11**, 67.
Weber, Th., Boysen, H., Frey, F. & Neder, R. B. (1997). *Acta Cryst.* B**53,** 544–552.
Weber, Th., Boysen, H., Honal, M., Frey, F. & Neder, R. B. (1996). *Z. Kristallogr.* **211**, 238–246.
Welberry, T. R. & Mayo, S. C. (1996). *J. Appl. Cryst.* **29**, 353–364.
Zernike, F. & Prins, J. A. (1927). *Z. Phys.* **41**, 184–194.